STATIC AND SEISMIC BEHAVIOUR OF STAINLESS STEEL WUF-B JOINTS

YIDU BU[1], YUANQING WANG[2], XUELIANG QIAO[3] and TIANXIONG ZHANG[4]

[1]*Civil Engineering Department, Tsinghua University, Beijing, China.*
E-mail: yidubu@tsinghu.edu.cn
[2]*Civil Engineering Department, Tsinghua University, Beijing, China.*
E-mail: wang-yq@tsinghua.edu.cn
[3]*Civil Engineering Department, Shenyang Jianzhu University, Shenyang, China.*
E-mail: qiaoxueliang1991@163.com
[4]*Civil Engineering Department, Tianjin University, Tianjin, China.*
E-mail: abcwow123@163.com

Stainless steel is being more commonly used in the construction due to its corrosion resistance and favorable material properties. Structures in corrosive environments may have lower maintenance cost if made from stainless steel compared to carbon steel, leading to a significant reduction in the whole life cost. While the behavior of various of types of joints made of carbon steel is well described in design codes, no such standard exists for stainless steel. This paper studies the structural behavior of welded unreinforced flanges, bolted web (WUF-B) joints, one of the most commonly used beam-to-column joints in mainland China steel constructions. A series of full-scale experimental studies of WUF-B joints was conducted, including one joint tested under monotonic loading and five under cyclic loading, representing the first characterization of the seismic behavior of these joints. All specimens were made of Grade S31608 (EN 1.4401) stainless steel welded I-sections. The results show that stainless steel WUF-B joints exhibit favorable seismic performance for use in corrosive and/or seismically active environments.

Keywords: Beam-to-column joint, moment-rotation behavior, stainless steel, test, WUF-B joint.

1 Introduction

The use of stainless steel is becoming increasingly common in civil and offshore engineering applications (Gardner 2019). This is not only due to its aesthetic appeal, but increasingly also due to the favorable anti-corrosive material properties of stainless steel, leading to a significant reduction in the whole life cost compared to carbon steel structures. The material stress-strain response as well as the structural response at the cross-section, member and frame levels have by now been extensively studied, showing that stainless steel differs from carbon steel in a number of ways; most importantly amongst them the non-linearity of the stress-strain behavior of stainless steel as compared to the linear/perfectly plastic behavior of carbon steel.

Studies of various types of stainless steel sections (I-sections, box sections, rectangular hollow sections) generally found that current design guidelines tend to be overly conservative (Gardner and Theofanous 2008, Yuan et al. 2014), due to the material non-linearity. The structural behavior of laser-welded stainless steel sections and members has been shown to be particularly beneficial (Gardner et al. 2016, Bu and Gardner 2019) with the favorable processing method of laser-welding. Similarly, studies have (both experimentally and numerically) investigated the behavior of stainless steel connections (Kim et al. 2008, Bouchaïr et al. 2008,

Proceedings of the 17th International Symposium on Tubular Structures.
Editors: X.D. Qian and Y.S. Choo

Published by Research Publishing, Singapore.
ISBN: 978-981-11-0745-0; doi:10.3850/978-981-11-0745-0_150-cd

Salih et al. 2010) and joints (Elflah et al. 2019a, 2019b, 2019c) and also reached to the conclusion that taking analogies with carbon steel design guide may neglect the high ductility and pronounced strain-hardening of stainless steel.

Regarding seismic behavior, the material and structural behavior of carbon steel is extensively studied, but the seismic behavior of stainless steel is much less investigated. Seismic performance of the material level has been studied and it was found that stainless steel exhibits various levels of cyclic hardening and high ductility (Wang et al. 2014, Chacón et al. 2018, Chang et al. 2019). Several numerical studies have also shown that structures under seismic loading exhibit enhanced performance in global ductility when stainless steel is incorporate in carbon steel structures as dissipative members (Sarno et al. 2003, Li et al. 2014). However, the benefit of implementing stainless steel in construction applications is subject to a number of constraints and design considerations, as has been pointed out in a recent experimental study of the seismic behavior of bolted extended end plate (BSEP) stainless steel joint (Bu et al. 2019), that stainless steel bolted assemblies needed to be specially treated to guarantee valid connections. Building on the authors' previous study of BSEP joints, this work explores the seismic performance of welded unreinforced flanges, bolted web (WUF-B) joints, which are commonly used as semi-rigid beam-to-column joints because of their ease of fabrication and erection. Both the static and the seismic performance of the joints were investigated in this paper.

2 Material behavior

Prior to the joint tests, the material properties of stainless steel plates have been tested. Joint specimens were made of grade S31608 (EN 1.4401) stainless steel. For each plate thickness (8 mm, 12 mm and 16 mm) of the tested joints, three tensile coupons were extracted parallel to the rolling direction. The dimensions of the coupons are designed following the tensile testing procedure set out in GB/T 228 (2002). The average key measured properties are presented in Table 1, including Young's modulus E, 0.2% proof stress f_y, ultimate tensile stress f_u, the strain hardening exponents for the compound Ramberg-Osgood (R-O) model n and $n'_{0.2,1.0}$.

Table 1. Material properties obtained from tensile coupon tests.

Thickness (mm)	E (MPa)	f_y (MPa)	$f_{1.0}$ (MPa)	f_u (MPa)	n	$n'_{0.2,1.0}$
8	203300	221	514	603	6.0	2.0
12	190407	228	486	593	6.5	2.5
16	193965	212	493	593	6.5	2.0

3 Joint tests

3.1 *Test specimens*

Six full-scale WUF-B joints were fabricated. A column of height 2300 mm with cross-section 450×250×12×16 ($h\times b\times t_w\times t_f$) was used in all cases. Two different beam cross-sections were employed, as tabulated in Table 2. These dimensions were designed based on typical single sided beam-to-column joints in multi-story steel frames, following the design guidance of GB 50017 (2017) and GB 50011(2010). Web connections were bolted to the beam with bolt arrangements designed to transfer the full strength of shear in the beam section, centered around the beam mid-depth. Three types of M24 bolts were used: Grade 8.8 high strength steel bolts, and austenitic stainless steel bolts A4-80 and A4-70. Shear-tab connections were used, consisting of a single plate welded perpendicular to the column flange and bolted with four or six bolts to the beam web. Their typical geometry is shown in Fig. 1. Complete joint penetration

(CJP) welds were used to connect the beam flange and the column flange on site. A summary of the parameters of each test specimen is given in Table 2, where JM1 represents joint number one under monotonic loading and JC1 under cyclic loading.

Table 2. Details of the designed specimens.

Specimen ID	Beam cross-section	Beam length (mm)	Bolt type	Number of bolts	Loading protocol
JM1	400×150×8×12	2000	A4-80	6	Monotonic loading
JC1	400×150×8×12	2000	A4-80	6	Cyclic loading
JC2	400×150×8×12	2000	8.8	6	Cyclic loading
JC3	400×150×8×12	2000	A4-70	6	Cyclic loading
JC4	300×200×8×12	1550	A4-80*	4	Cyclic loading
JC5	300×200×8×12	1550	A4-80	4	Cyclic loading

*The shear tab of JC4 is welded to the beam web, such that the bolts are only used for positioning.

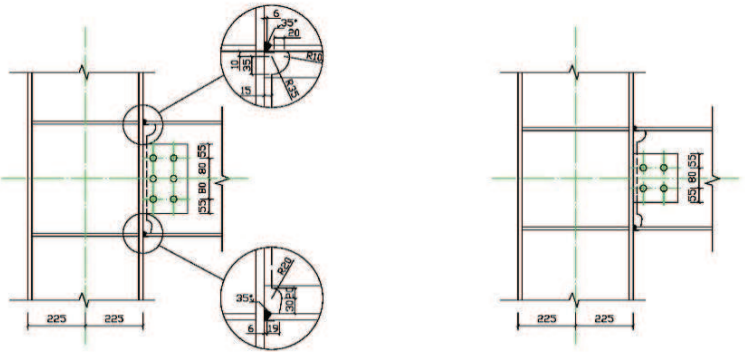

(a) Six-bolts arrangement (b) Four-bolts arrangement

Figure 1. Typical layout of the bolt connections (in mm).

3.2 *Test setup and instrumentation*

The tests under monotonic and cyclic loading were using the same test setup, as shown in Fig. 2. The columns were clamped 150 mm inward from both ends by anchor bolts, leaving the length between the anchor bolts 2000 mm. The right end of the column was fixed while the left end of the column was connected to 500 kN load cell which applied axial load to the column. A 500 kN actuator was connected to the end of the beam to apply monotonic or cyclic loading. The horizontal loading was applied 200 mm inward from the free end of the beam through a special bracket which restrict the loading in plane. Two cables which were connected to the bracket and mounted to the floor on each side were used to assist the loading in-plain. All bolts were fastened with preload using the torque wrench method, with Grade 8.8 preloaded to 140 kN, according to JGJ82 (2011), while A4-70 and A4-80 preloaded to the level reduced by the proof strength ratio.

LVDTs were used to monitor the displacements at three locations of the specimens, as shown in Fig. 2. L1 measured the horizontal displacement at the beam loading point. L2 and L3 measured the in-plane vertical displacement on the column outside the connection area, namely the rigid body motion of the joint. The LVDT readings were used to calculate the rotation of the

joint. All instrumentation was connected to a data acquisition system and readings were recorded every second.

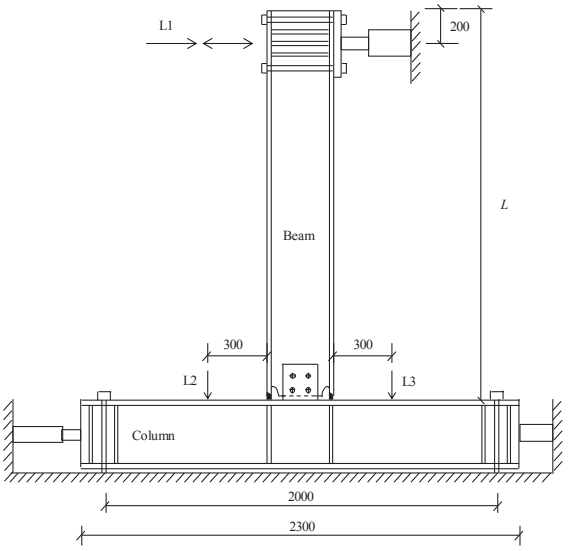

Figure 2. Test setup.

At the beginning of the tests, the axial load of the column was first applied by the load cell at 300 kN and kept constant during the remainder of the test. The free end of the beam was under displacement control at a rate of 1.5 mm/min for monotonic loading. For specimens under cyclic loading, the specimens were tested under load control and the loading scheme was designed in accordance with JGJ101(2015), characterized by the occurrence of significant yield.

3.3 *Test results*

3.3.1 *Failure modes*

The failure modes from the tests are presented in Fig. 3. Specimen JM1 under monotonic loading responded elastically up to moment level about 300 kNm. Buckling of the flanges under compression was observed and the test were terminated due to significant joint rotations, inelastic deformations and loss of stiffness. At the end of the tests a small crack was observed on the weld surface of the tensile flange of the beam.

All specimens under cyclic loading (JC1-JC5) have shown similar failure modes: cracks initiated in various locations, following which the beam flange experienced different levels of local buckling. Finally, fracture failure of the weld in corresponding locations occurred, including the fracture of the CJP welds between the beam flanges and the column flanges, fracture of the welds between the column flanges and the column webs in the joint region, fracture of the welds between the beam flanges and the beam webs. The welded steel elements contained discontinuities and high stress concentrations at weld toes. The fatigue process includes the formation and propagation of a crack under repeated loads, leading to final fracture when the remaining un-cracked section can no longer carry the loads experienced by the structure. Brittle failure modes of the joints and failure in the column should be avoided through design considerations. Welding quality exhibits higher impact on the low cycle fatigue characteristics of stainless steel joints, since the welds should be ductile enough to take advantages of the high level of ductility and strain hardening of stainless steel.

After the tests, the bolts were removed from the specimens. The bolts in JC4 are only for positioning while the welds between the shear tab and the beam web are transferring shear load, thus no visible deformation can be observed. For all test specimens apart from JC4, plastic deformation can be observed at the bolt holes, showing that the preloaded bolts did not maintain slip-resistant at ultimate limit state and behaved as bearing type connections.

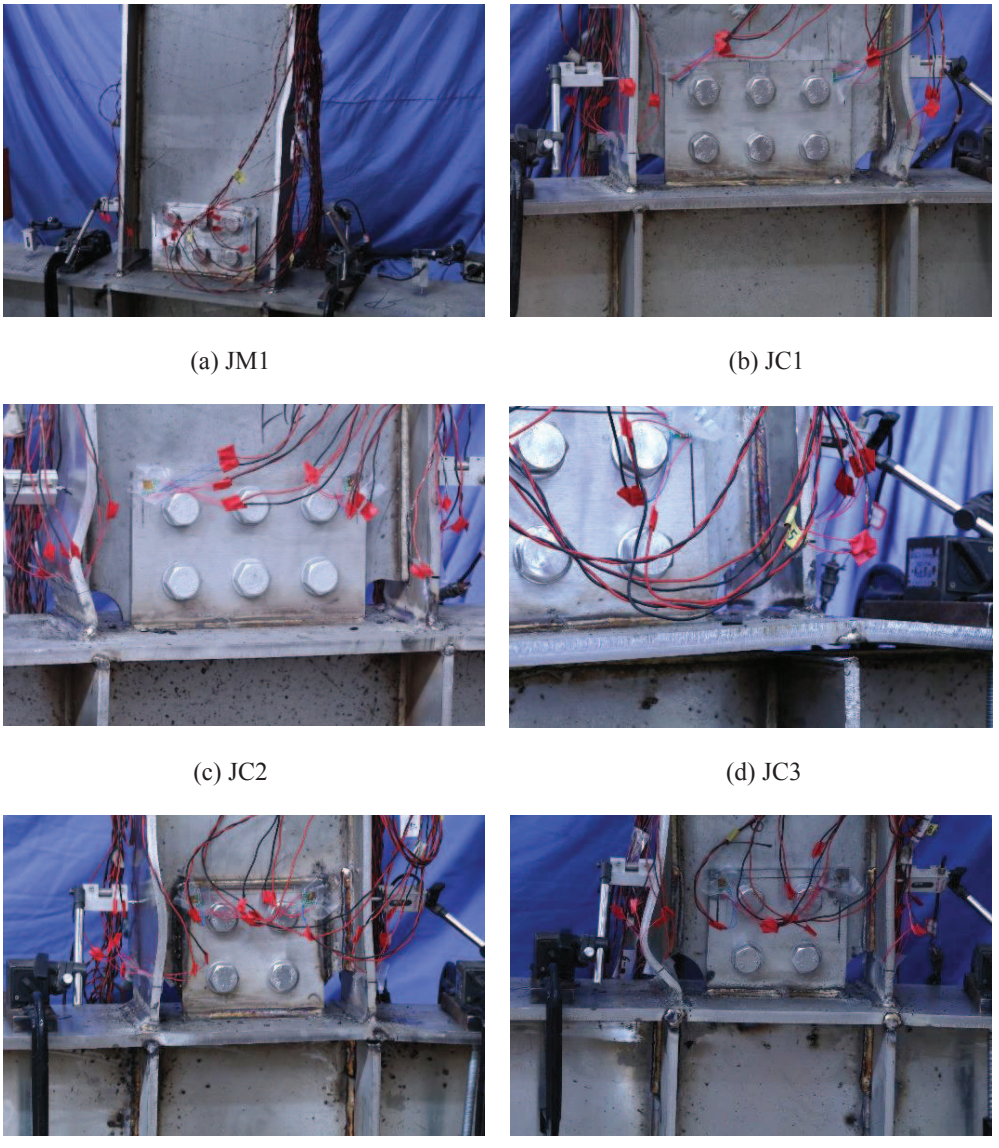

(a) JM1 (b) JC1

(c) JC2 (d) JC3

(e) JC4 (f) JC5

Figure 3. Failure modes.

3.3.2 *Moment-rotation responses*

Moment-rotation curves describe the relationship between the bending moment M applied to a joint and the corresponding rotation φ between the connected members, revealing the rotational behavior of a joint. The moment acting on the joint was determined by multiplying the force

applied on the beam end by the distance of the actuator from the column face. The joint rotation φ was calculated from the LVDT readings.

$$\varphi = \frac{\delta_1}{L} - \frac{\delta_2 - \delta_3}{D} - \theta_{b,el}$$

where δ_1 (the reading of LVDT1) is the displacement at the loading point, δ_2 and δ_3 (readings of LVDT2 and LVDT3) measured the rigid body motion of the joint. L is the measured distance from the loading point on the beam to the surface of the column, D is the measured distance between LVDT2 and LVDT3, and $\theta_{b,el}$ is the elastic rotation of the beam according to the beam theory. In this way the rotation caused by the rigid body motion of the joint and the elastic deformation of the beam was excluded.

The moment-rotation curves (M-φ) of all the tested joints (JM1, JC1 to JC5) are shown in Fig. 4. It can be seen that the hysteretic loops of all the specimens under seismic loading were plump shuttle shaped. Skeleton curves of the joints under cyclic loading are presented with the moment-rotation curve of joint JM1 in Fig. 5. Two dashed lines outline the area of semi-rigidity of the joint should it be employed in the unbraced multi-story steel frame design protocol (of the same height and span). The parameters obtained from the moment-rotation curves are concluded in Table 3, including the plastic moment resistance M_j, the maximum moment M_m, rotation φ_m corresponding to the maximum moment, maximum recorded rotation φ_f and the initial stiffness $S_{j,ini}$.

From Table 3 it can be seen that all specimens show good ductility. The initial stiffness and maximum moment of JM1, JC1, JC2 and JC3 are similar due to similar geometry of the joints. The behavior did not reflect different bolt types since the failure of the bolts was after the failure of the welds. JC4 has slightly higher initial stiffness and less ductility, compared to JC5, because the shear tab of JC4 was welded to the beam web.

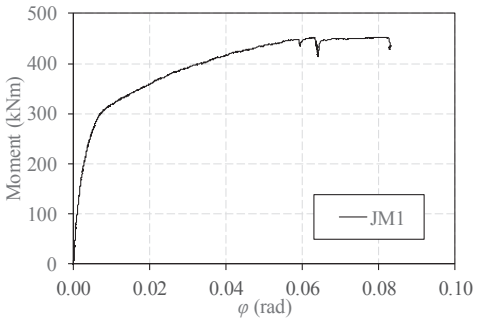

(a) JM1

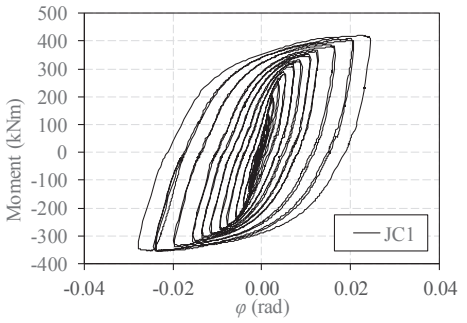

(b) JC1

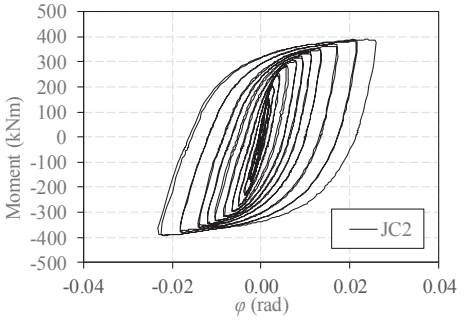

(c) JC2

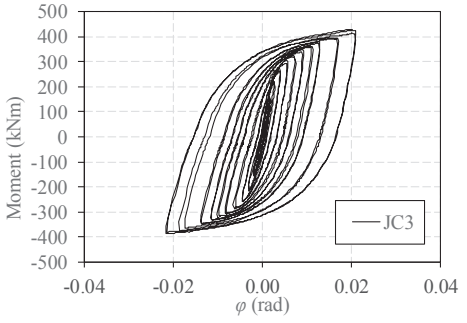

(d) JC3

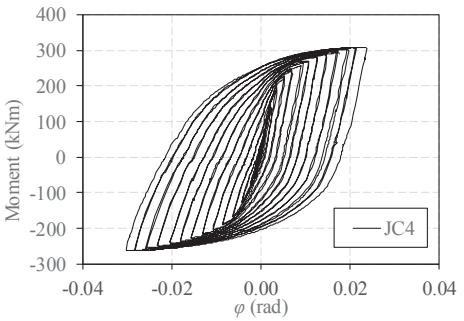

(e) JC4

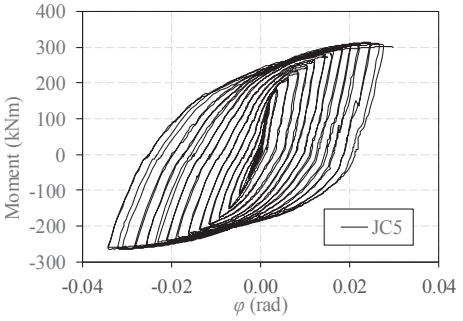

(f) JC5

Figure 4. Moment rotation curves.

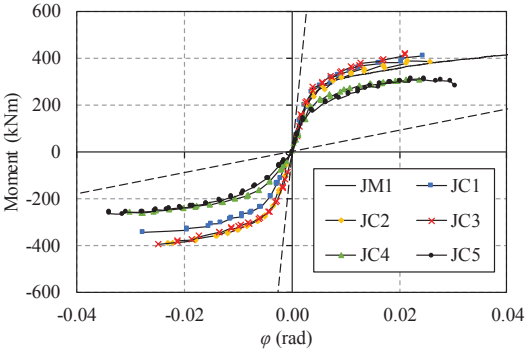

Figure 5. Skeleton curves.

Table 3. Test results.

Specimens ID	M_j (kNm)	M_m (kNm)	φ_m (mrad)	φ_f (mrad)	$S_{j,ini}$ (kNm/mrad)
JM1	261.111	452.952	78.391	83.326	97.085
JC1	275.000	419.553	21.837	27.788	81.395
JC2	277.778	391.725	21.137	25.744	76.269
JC3	277.778	429.298	19.811	21.686	89.616
JC4	211.111	309.275	21.277	30.216	50.073
JC5	213.889	314.840	24.585	34.217	39.246

4 Conclusions

An experimental study has been conducted to investigate the static and seismic behavior of stainless steel WUF-B joints. Six full-scale stainless steel beam-to-column joint tests were carried out, including one joint under monotonic loading and five under seismic loading. The testing configuration and obtained test results are reported. The joints failed mainly due to weld failure accompanied with extensive inelastic deformations of the beam flange. The results show that stainless steel WUF-B joints exhibit favorable seismic performance for use in corrosive and/or seismically active environments. The quality of the welds and the shape of the weld access hole also controls the behavior of the joints.

Acknowledgements

The financial support received from the National Natural Science Foundation of China (No. 51878377) is gratefully acknowledged. The authors would like to thank Dongge for the supply of test specimens.

References

Bouchaïr, A., Averseng, J. and Abidelah, A., Analysis of the Behaviour of Stainless Steel Bolted Connections, J. Constr. Steel Res., 64, 1264–1274, Nov, 2008.

Bu, Y. and Gardner, L., Finite Element Modelling and Design of Welded Stainless Steel I-Section Columns, *J. Constr. Steel Res.,* 152, 57–67, Jan, 2019.

Bu, Y., Wang, Y. and Zhao, Y., Study of Stainless Steel Bolted Extended End Plate Joints under Seismic Loading. *Thin Walled Struct.*, 144, Nov, 2019.

Chacón, R., de Marco, M., Real, E. and Arrayago, I., An Experimental Study on the Cyclic Response of Austenitic Stainless Steel, in *Ninth International Conference in Steel Structures (ICASS2018),* Chan, S. L.(ed.), Hong Kong 2018.

Chang, X., Yang, L., Zong, L., Zhao, M. H., Yin, F., Study on Cyclic Constitutive Model and Ultra Low Cycle Fracture Prediction Model of Duplex Stainless Steel. *J. Constr. Steel Res.,* 152:105-116. Jan, 2019.

Di Sarno, L., Elnashai, A. S. and Nethercot, D. A., Seismic Performance Assessment of Stainless Steel Frames. *J. Constr. Steel Res.,* 59(10), 1289-1319, Oct, 2003.

Elflah, M., Theofanous, M., Dirar, S. and Yuan, H., Behaviour of Stainless Steel Beam-to-Column Joints - Part 1: Experimental Investigation, *J. Constr. Steel Res.,* 152, 183–193, Jan, 2019a.

Elflah, M., Theofanous, M. and Dirar, S., Behaviour of Stainless Steel Beam-to-Column Joints-Part 2: Numerical Modelling and Parametric Study, *J. Constr. Steel Res.,* 152, 194–212, Jan, 2019b.

Elflah, M. , Theofanous, M. , Dirar, S. and Yuan, H., Structural Behaviour of Stainless Steel Beam-to-Tubular Column Joints. *Eng. Struct.,* 184, 158-175, Apr, 2019c.

Gardner, L. and Theofanous, M., Discrete and Continuous Treatment of Local Buckling in Stainless Steel Elements, *J. Constr. Steel Res*., 64, 1207–1216, Nov, 2008.

Gardner, L., Bu, Y., and Theofanous, M., Laser-Welded Stainless Steel I-Sections: Residual Stress Measurements and Column Buckling Tests, *Eng. Struct.,* 127, 536–548, Nov, 2016.

Gardner, L., Stability and Design of Stainless Steel Structures – Review and Outlook, *Thin Walled Struct.*, 141, 208–216, Apr, 2019.

GB/T 228.1, *Metallic Materials-Tensile Testing-Part 1: Method of Test at Room Temperature,* Standards Press of China, Beijing, 2011.

GB 50017-2017, *Code for Design of Steel Structures,* China Planning Press, Beijing, 2017 (in Chinese).

GB 50011-2010, *Code for Seismic Design of Buildings,* China Architecture and Building Press, Beijing, 2010 (in Chinese).

JGJ 82-2011, *Technical Specification for High Strength Bolt Connections of Steel Structure.* China Architecture and Building Press, Beijing, 2011 (in Chinese).

JGJ/T 101-2015, *Specification for Seismic Test of Buildings,* China Architecture and Building Press, Beijing, 2015 (in Chinese).

Kim, T. S., Kuwamura, H., and Cho, T. J., A Parametric Study on Ultimate Strength of Single Shear Bolted Connections with Curling, *Thin-Walled Struct.*, 46, 38–53, Jan 2008.

Li, R, Zhang, Y., Tong, L. W., Numerical Study of The Cyclic Load Behavior of AISI 316L Stainless Steel Shear Links for Seismic Fuse Device. *Front. Struct. Civ. Eng.,* 8 (4), 414-426, Sep, 2014.

Salih, E. L., Gardner, L. and Nethercot, D. A., Numerical Investigation of Net Section Failure in Stainless Steel Bolted Connections, *J. Constr. Steel Res.,* 66 (12), 1455–1466, Dec, 2010.

Wang, Y. Q., Chang, T., Shi, Y. J., Yuan, H. X., Yang, L. and Liao, D. F., Experimental Study on the Constitutive Relation of Austenitic Stainless Steel S31608 under Monotonic and Cyclic Loading, *Thin Walled Struct.,* 83, 19–27, Oct, 2014.

Yuan, H. X., Wang, Y. Q., Gardner, L. and Shi, Y. J., Local-Overall Interactive Buckling of Welded Stainless Steel Box Section Compression Members, *Eng. Struct.,* 67, 62–76, May, 2014.